Dynamic Modeling of a Reformed Methanol Fuel Cell System using Empirical Data and Adaptive Neuro-Fuzzy Inference System Models

Justesen, Kristian Kjær; Andreasen, Søren Juhl; Shaker, Hamid Reza

Published in:
Journal of Fuel Cell Science and Technology

DOI (link to publication from Publisher):
10.1115/1.4025934

Publication date:
2014

Document Version
Publisher's PDF, also known as Version of record

Dynamic Modeling of a Reformed Methanol Fuel Cell System Using Empirical Data and Adaptive Neuro-Fuzzy Inference System Models

Kristian K. Justesen
e-mail: kju@et.aau.dk

Søren Juhl Andreasen
Associate Professor
e-mail: sja@et.aau.dk

Hamid Reza Shaker
Assistant Professor
e-mail: shr@et.aau.dk

Department of Energy Technology,
Aalborg University,
Aalborg East 9220, Denmark

In this work, a dynamic MATLAB Simulink model of an H3-350 reformed methanol fuel cell (RMFC) stand-alone battery charger produced by Serenergy® is developed on the basis of theoretical and empirical methods. The advantage of RMFC systems is that they use liquid methanol as a fuel instead of gaseous hydrogen, which is difficult and energy-consuming to store and transport. The models include thermal equilibrium models of the individual components of the system. Models of the heating and cooling of the gas flows between components are also modeled and adaptive neuro-fuzzy inference system models of the reforming process are implemented. Models of the cooling flow of the blowers for the fuel cell and the burner which supplies process heat for the reformer are made. The two blowers have a common exhaust, which means that the two blowers influence each other's output. The models take this into account using an empirical approach. Fin efficiency models for the cooling effect of the air are also developed using empirical methods. A fuel cell model is also implemented based on a standard model, which is adapted to fit the measured performance of the H3-350 module. All of the individual parts of the model are verified and fine-tuned through a series of experiments and are found to have mean absolute errors between 0.4% and 6.4% but typically below 3%. After a comparison between the performance of the combined model and the experimental setup, the model is deemed to be valid for control design and optimization purposes.
[DOI: 10.1115/1.4025934]

1 Introduction

Polymer electrolyte membrane (PEM) fuel cells have been found to have a wide range of applications in both mobile and stationary systems. They do, however, have a problem with the heavy and space consuming storage of its hydrogen fuel. This being in the form of high pressure tanks or in liquid form at a temperature below $-252.87\,^{\circ}\mathrm{C}$. A fuel which is liquid at ambient temperature and pressure would be a great advantage. Methanol is such a fuel and reformed methanol fuel cell (RMFC) systems are, therefore, of great interest and the focus of this work is the dynamic modeling of a H3-350 stand-alone RMFC battery charger module developed by Serenergy®. The rated output power of the module is 350 W and the external dimensions are $279 \times 204 \times 595$ mm, not including a fuel tank. The weight of the module is 13.7 kg and more information about the module can be found on the Serenergy® web page [1]. Figure 1 shows a picture of an H3-350 module.

In an RMFC system, methanol is reformed into a hydrogen rich gas in a reformer and fed to a fuel cell. The fuel cell uses some of the hydrogen in the reformed gas and the other components of the gas flow through the fuel cell stack as exhaust. Several different reformation processes exist but the H3-350 module uses steam reformation, where methanol and water is reformed on a suitable catalyst at temperatures between 240 °C and 300 °C. Equation (1) shows the steam reformation reaction [2]

$$\mathrm{CH_3OH} + \mathrm{H_2O} \rightleftharpoons 3\mathrm{H_2} + \mathrm{CO_2}(49.5\ \mathrm{kJ/mol}) \tag{1}$$

This is an endothermic reaction and requires an energy supply of 49.5kJ/mol. This is, however, not the only process which takes place in the reformer. A methanol decomposition reaction also takes place, according to Eq. (2)

$$\mathrm{CH_3OH} \rightleftharpoons 2\mathrm{H_2} + \mathrm{CO}(90.7\ \mathrm{kJ/mol}) \tag{2}$$

This reaction is less dominant and undesirable because it creates carbon monoxide, which is harmful to PEM fuel cells. Some of this carbon monoxide is removed by the water gas shift reaction given in Eq. (3)

$$\mathrm{CO} + \mathrm{H_2O} \rightleftharpoons \mathrm{H_2} + \mathrm{CO_2}(-41\ \mathrm{kJ/mol}) \tag{3}$$

The rate at which these reactions occur is dependent upon the temperature of the reformer bed, the type and amount of catalyst present, the relationship between the water and the methanol in the fuel (steam to carbon ratio), and the fuel mass flow.

As previously mentioned, the carbon monoxide in the reformed gas can be harmful to PEM fuel cells, in general, and low temperature PEM (LTPEM) fuel cells in particular. A gas cleanup stage, therefore, has to be implemented in an RMFC system if an LTPEM fuel cell is used [3,4]. The H3-350 module, which is the subject of this work, therefore uses a high temperature PEM (HTPEM) fuel cell, which has a higher carbon monoxide tolerance [5–7].

The HTPEM fuel cell in the H3-350 module is air-cooled and the high temperature exhaust air is used to heat and evaporate the fuel in a heat exchanger, which is known as the evaporator.

Contributed by the Advanced Energy Systems Division of ASME for publication in the JOURNAL OF FUEL CELL SCIENCE AND TECHNOLOGY. Manuscript received September 4, 2013; final manuscript received October 17, 2013; published online December 4, 2013. Editor: Nigel M. Sammes.

Fig. 1 Picture of the integrated H3-350 RMFC stand-alone battery charger developed by Serenergy®

When a PEM fuel cell is operated on reformed gas where the hydrogen is mixed with other gases, a constant flow of fuel through the fuel cell is necessary. In addition, an anode over stoichiometry is necessary to avoid starvation of the fuel cell, which leads to degradation. In the H3-350 module this over stoichiometry is fed to a catalytic burner which then supplies all of the process heat for the reformer. The temperature of the reformer is controlled using a blower, which also supplies process air for the burner. Each component is equipped with an electric heater, which is used during the system startup procedure. Figure 2 shows a diagram of the H3-350 module.

The highly integrated construction of the module means that none of the module's output power has to be used to heat, evaporate, and reform the fuel. This leads to a higher system efficiency. It does, however, lead to a higher system complexity and several internally coupled energy flows. This means that constructing accurate system models for control and optimization purposes becomes more difficult, but yet more crucial.

In this work the development of a dynamic MATLAB Simulink model is described as along with the identification methods used to fill in the model parameters and the final model verification.

Some of the models are physical models which contain physical values such as weight, heat capacity, mass flow, and energy flows. But other models will be empirical models which contain nonphysical and physical parameters. This leads to a loss of generality, which means some of the identification experiments must be redone if changes are made to the module. This makes it hard to use the model for physical model optimization. It is, however, very useful for controller design and for an analysis of the module's performance at different operating points.

2 Modeling and System Identification

This section describes the structure of the developed MATLAB Simulink model and the individual parts of the model, the identification experiments, and the procedures used to identify the model parameters.

2.1 Lumped Thermal Masses. The components of the system are modeled as lumped thermal masses with energy flows going to and from them. Figure 3 illustrates this concept for the burner and reformer, which are modeled as two separate masses connected by a temperature driven energy flow.

This method has the weakness that the temperature gradients through the components of the system are not modeled. An analysis of the model output will determine if it is sufficiently accurate for control and optimization purposes. The temperature of the reformer can be calculated as

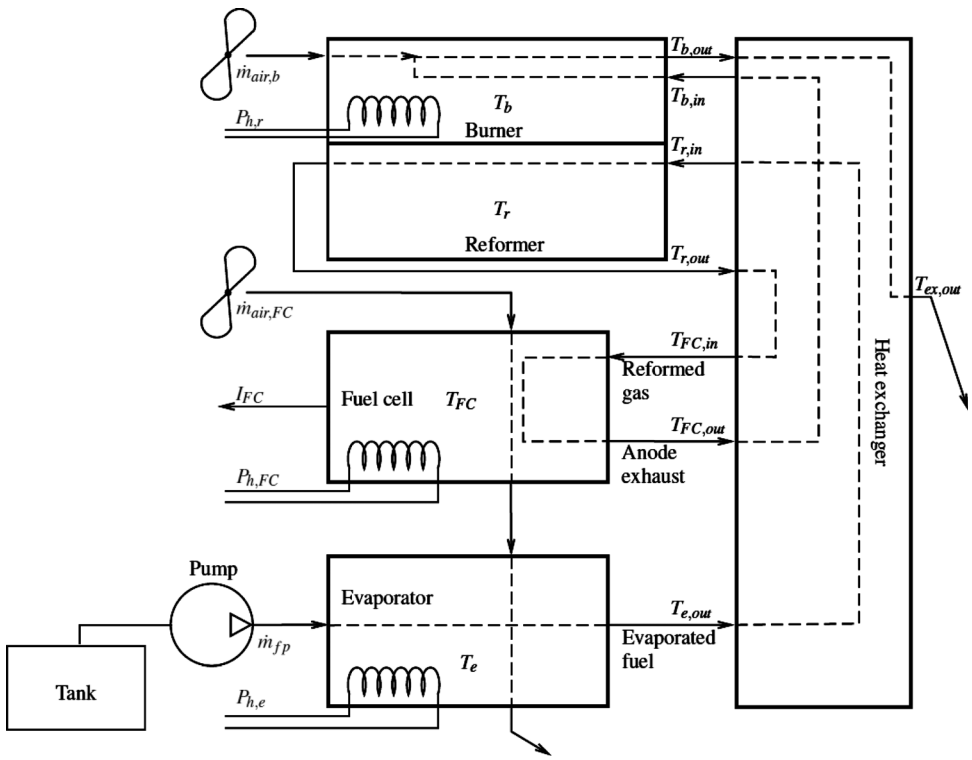

Fig. 2 Overview of the H3-350, with indication of the modeled temperatures, printed in black, and the directly controllable parameters gathered to the left in the figure, printed in gray

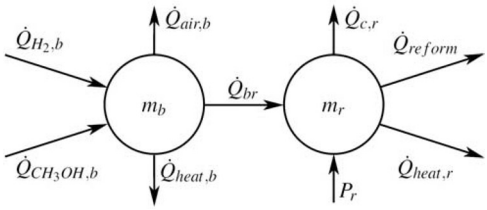

Fig. 3 Thermal model of the burner and reformer

$$T_r = \frac{1}{m_r \cdot Cp_r}\int(\dot{Q}_{\text{br}} - \dot{Q}_{h,r} - \dot{Q}_{\text{reform}} - \dot{Q}_{c,r} + P_{h,r}) \cdot dt \quad (4)$$

where m_r is the mass of the reformer and Cp_r is the specific heating capacity of the reformer. Here, $\dot{Q}_{\text{br}}$ is the power transmitted from the burner to the reformer through the bulk material, driven by a difference in temperature and modeled as a first order relation on the basis of experimental data. This is the only direct thermal communication between the components of the module. In Eq. (4), $P_{h,r}$ is the heating power supplied by the electric heater and $\dot{Q}_{c,r}$ is the heat lost to the surroundings through conduction through the insulation of the module. This is assumed to be the only heat loss due to conduction. It is assumed that the fuel is heated to the reformer's temperature and $\dot{Q}_{h,r}$ is the power needed to do this. Finally, $\dot{Q}_{\text{reform}}$ is the power used to reform the fuel. The temperature of the burner can be calculated as

$$T_b = \frac{1}{m_b \cdot Cp_b}\int(\dot{Q}_{\text{H}_2,b} + \dot{Q}_{\text{CH}_3\text{OH},b} - \dot{Q}_{h,b} - \dot{Q}_{\text{air},b} - \dot{Q}_{\text{br}}) \cdot dt \quad (5)$$

where m_b is the mass of the burner and Cp_b is the specific heating capacity of the burner, $\dot{Q}_{\text{H}_2,b}$ is the power supplied by the burning of hydrogen in the catalytic burner, and $\dot{Q}_{\text{CH}_3\text{OH},b}$ is the power supplied by burning the methanol, which parses through the reformer unreformed. It is assumed that all of the hydrogen and methanol is burned. It is assumed that the gas going into the burner is heated to the burner's temperature and $\dot{Q}_{h,b}$ is the power used to do this. Finally, $\dot{Q}_{\text{air},b}$ is the cooling effect of the air supplied by the blower. The temperature of the fuel cell can be calculated as

$$T_{\text{FC}} = \frac{1}{m_{\text{FC}} \cdot Cp_{\text{FC}}}\int(P_{\text{loss,FC}} + P_{h,\text{FC}} - \dot{Q}_{\text{heat,FC}} - \dot{Q}_{\text{air,FC}} - \dot{Q}_{c,\text{FC}}) \cdot dt \quad (6)$$

where m_{FC} is the mass of the fuel cell, Cp_{FC} is the specific heating capacity of the fuel cell, $P_{\text{loss,FC}}$ is the loss in the fuel cell which is converted into heat, and $P_{h,\text{FC}}$ is the heating power supplied by the electric heater in the fuel cell. It is assumed that the gas parsing through the fuel cell is cooled to the fuel cell's temperature and $\dot{Q}_{\text{heat,FC}}$ is the power transferred to the fuel cell as a result of this process. Here, $\dot{Q}_{\text{air,FC}}$ is the cooling power of the air from the blower and $\dot{Q}_{c,\text{FC}}$ is the heat lost through conduction through the module's insulation. The temperature of the evaporator is calculated as

$$T_e = \frac{1}{m_e \cdot Cp_e}\int(P_{h,e} + \dot{Q}_{\text{air},e} - \dot{Q}_{h,e} - \dot{Q}_{c,e}) \cdot dt \quad (7)$$

where m_e is the mass of the evaporator, Cp_e is the heating capacity of the evaporator, $P_{h,e}$ is the heating power from the electric heater in the evaporator, $\dot{Q}_{\text{air},e}$ is the heat supplied to the evaporator from the fuel cell exhaust air, $\dot{Q}_{h,e}$ is the power used to heat and evaporate the fuel coming into the evaporator, and $\dot{Q}_{c,e}$ is the heat lost due to conduction through the module's insulation.

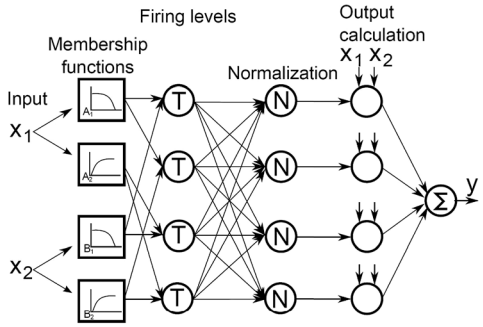

Fig. 4 ANFIS model structure used in this work [9]

2.2 Modeling the Reforming Process. To be able to predict the performance of the module, it is important to know the composition of the reformed gas under different conditions. By observing the reactions in Eqs. (1)–(3), it is determined that the models should be of the mass flow of hydrogen, carbon dioxide, carbon monoxide, and methanol which goes through the reformer unreformed. From these models the mass flow of water can be calculated. Here, mass flow is chosen to describe the gas flow but molar flow could also be used. In this work a method based on adaptive neuro-fuzzy inference systems (ANFISs), originally developed in Ref. [8] is used. A more in-depth description of the mass flow models and how they are constructed can be found in Ref. [9], but a brief description of the models is given here.

An ANFIS is a neuro-fuzzy modeling approach which can be trained on experimental data to behave like a physical system. Figure 4 shows the ANFIS modeling structure used in this work.

The ANFIS structure consists of five layers. The first layer is the fuzzyfication layer, where the crisp input signals are converted into fuzzy variables by determining their degree of membership to a number of fuzzy sets. Here, the fuzzy sets can be the terms high or low temperature or low temperature or flow. Where the membership of a normal set can be described using crisp variables, 1 or 0, the membership of a fuzzy set is described using a fuzzy variable which can take values between 1 and 0. The number of membership functions associated with each input determines the complexity of the models and, thereby, its ability to model nonlinear correlations between the inputs and the output. The factors which determine the shape of the membership functions are adaptive and are changed during the tuning of the ANFIS models. Each of the nodes in the second layer denotes the beginning of the calculation of a fuzzy rule. In the second layer,the firing levels of the different rules are determined. The firing level of a rule describes to which degree the fuzzy input variables are high, i.e., to which degree the inputs belong to the fuzzy sets in question. In the third layer, the firing levels are normalized. The operations in these two layers are nonadaptive. In the fourth layer, the contributions of each rule to the output of the model is calculated. Each node in the layer contains three adaptive parameters which are changed during the tuning of the models. In the fifth layer, the contributions of the individual rules are summed to give the output of the models.

A series of experiments where the fuel cell of the module is replaced by a gas analyzer is performed. The gas analyzer used in the experiment consists of four modules: a Siemens Fidamat 6 which is used to measure the methanol content in the gas, a Siemens Ultramat which measures the carbon dioxide and carbon monoxide content, and a Siemens Calomat 6 which measures the hydrogen content.

The measurements were performed over a 26 h period with a reformer temperature which is stepped from 240 °C to 300 °C in increments of 10 °C. At each temperature the flow starts at 200 mL, it is then changed to 250 mL, 300 mL, 350 mL, 400 mL, and 450 mL. The flow is then returned to the starting point through the same steps to investigate any hysteresis effects.

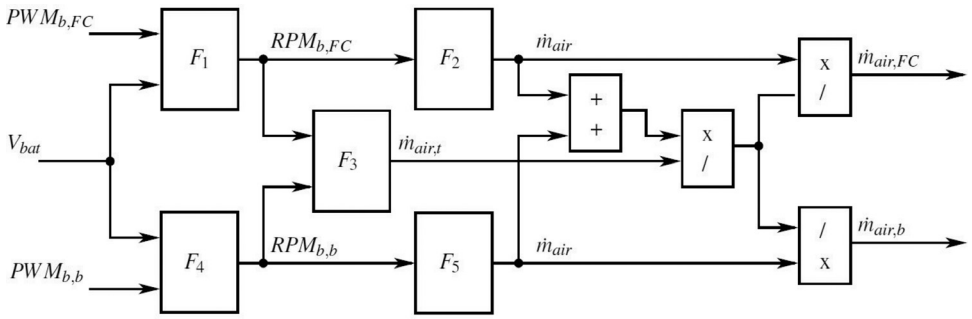

Fig. 5 Blower model, PWM to air mass flow

The inputs to the models are the reformer temperature and the fuel flow because these are the factors which are expected to influence the gas composition. Different numbers of membership functions have been tried and the results have been compared using the mean absolute error (MAE), which is calculated as

$$\text{MAE} = \frac{1}{n} \cdot \sum_{i=1}^{n} |e_i| \tag{8}$$

where e is the error between the measured and modeled values and n is the number of samples. It can be hard to set a maximum allowable MAE which applies to all models, since the complexity of the variable which is to be modeled and the quality of the measurements limits the accuracy of the models. The MAE of the models developed in this work is, therefore, assessed as the models are developed.

It was found that using three membership functions has the best balance between complexity and performance for the hydrogen and carbon dioxide model. They display MAEs of 0.7% and 0.71%, respectively. For the carbon monoxide and methanol slip models, four membership functions proved the best compromise, yielding MAEs of 6.4% and 4.56%, respectively. The larger error of these models is due to measurement noise but all of the models are considered valid for use in the dynamic model.

2.3 Blower Models. To model the cooling effects of the blowers it is important to know how much air is moved by the blowers. This is complicated because the two blowers have a common exhaust and the flow of one blower affects the other. The blowers are powered by the battery the module is charging. This means that the supply voltage for the blowers changes with the state of charge of the batteries. In addition, the correlation between the speed of the blowers and the airflow is dependent upon the pressure the blower works against, which is not measured in the physical system. The addition of extra pressure sensors is undesirable, since it would increase the cost and complexity of the module.

A series of empirical models are, therefore, constructed based on identification experiments which cover the operating ranges of the blowers. Figure 5 shows how these models are combined.

The first models F_1 and F_4 calculate the rotational speed of the blowers based on the battery voltage and the pulse width modulation (PWM) signals, which are sent to the blowers by some control algorithm. Equation (9) shows the linear regression approach used to determine the empirical factors in the following models:

$$\hat{\vartheta} = \left(\phi^T \cdot \phi\right)^{-1} \cdot \phi^T \cdot y \tag{9}$$

Here, $\hat{\vartheta}$ is the vector of parameters which are to be determined, ϕ is a vector containing the measured values upon which the model's output is dependent, and y is a vector containing the desired results.

Models where the rotational speed of the blowers was dependent on the battery voltage, the blower PWM signal, and the blower PWM signal squared were found to give the best fit. These have MAEs of 1.17% and 0.98% and are deemed to be valid.

The next two models F_2 and F_5 calculate the mass flows of the blowers on the basis of their rotational speed when they are operated on their own. The mass flow, in kg/s, is found by measuring the airspeed of the exhaust air and using the following equation:

$$\dot{m}_{\text{air}} = a_{\text{exhaust}} \cdot v_{\text{air}} \cdot \rho_{\text{air}} \tag{10}$$

where a_{exhaust} is the area of the exhaust pipe measured in m^2, v_{air} is the airspeed measured in m/s, and ρ_{air} is the density of the supplied air in kg/m^3. Models which use the rotational speed of the blowers and the rotational speed of the blowers squared as inputs were found to give the best fit. These have MAEs of 1.44% and 3.9%, respectively.

The F_3 model calculates the total gas flow when both blowers are on, using the same principle as the other mass flow models. It is observed that this flow is always lower than the flow when the two blowers are independently operated. It is assumed that the difference is distributed evenly between the two blowers and the mass flow reduction ratio is calculated and the individual mass flows are divided by it. Models where the rotational speeds of both blowers and the rotational speeds of both blowers squared are used as inputs were found to have the best fit. This model has an MAE of 2.10%.

Based on the low MAEs of the individual submodels, the blower models are deemed to be valid.

2.4 Electrical Fuel Cell Model. The fuel cell in the module is of the HTPEM type and contains 45 cells with a surface area of 45.16 cm^2 each. As mentioned in the Introduction, the HTPEM fuel cells have a relatively high tolerance to carbon monoxide and Serenergy® specifies that their fuel cells can be operated with carbon monoxide concentrations of up to 5% [1]. The gas composition experiments show that the highest carbon monoxide content of the reformed gas is 1%.

The electrical fuel cell model used in this work is from Ref. [10]. This model takes the cathode air stoichiometry, anode hydrogen stoichiometry, carbon monoxide concentration, fuel cell current, and fuel cell temperature into account. The output of the model is the fuel cell voltage under the given conditions.

Using this model directly and comparing its output with the fuel cell voltage measured in the experiments yields an MAE of 7.88%. The original model includes the effect of carbon monoxide in the fuel, but it does not take into account the water content of the reformed gas. Therefore, a term which is dependent on the water content and the fuel cell current is developed using linear regression. When this term is included, the MAE of the fuel cell model becomes 0.4%. Figure 6 shows the measured and simulated fuel cell voltage during a series of changes in the fuel cell current and temperature.

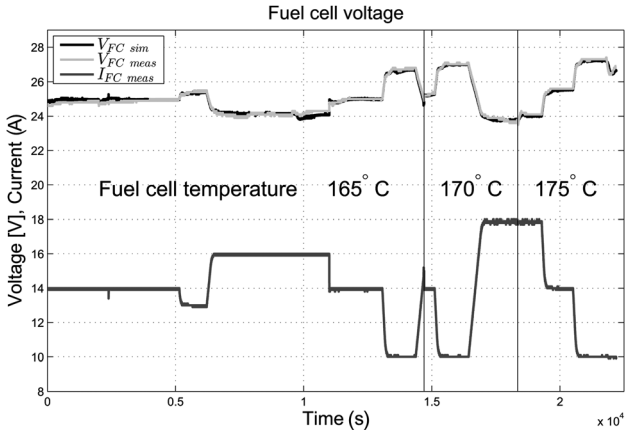

Fig. 6 Simulated and measured fuel cell voltage with extra model term

The energy lost as heat in the fuel cell $P_{\text{loss,FC}}$ in Eq. (6) is modeled as the difference between the lower heating value of the consumed hydrogen and the output power. The hydrogen consumption of the fuel cell, measured in kg/s, is calculated using

$$\dot{m}_{\text{H}_2\text{FC}} = \frac{N_{\text{cell}} \cdot M_{\text{H}_2}}{2 \cdot F} I_{\text{FC}} \tag{11}$$

where N_{cell} is the number of cells in the fuel cell stack, M_{H_2} is the molar weight of hydrogen in kg/mol, F is Faraday's constant measured in C/mol, and I_{FC} is the fuel cell current measured in A or C/s. This equation is also used when calculating the gas composition of the anode exhaust gas.

2.5 Fin Efficiency Models. The maximum possible cooling effect from an airflow is achieved if the air is heated to the temperature of the item it is cooling. For the burner, this maximum cooling effect is described by

$$\dot{Q}_{\text{air},b\,\max} = (T_b - T_a) \cdot Cp_{\text{air}} \cdot \dot{m}_{\text{air},b} \tag{12}$$

where T_a is the ambient temperature, Cp_{air} is the heating capacity of air, and $\dot{m}_{\text{air},b}$ is the mass flow of the cooling air. In practice, the temperature of the exhaust is lower than the temperature of the burner. This difference can be modeled using a fin efficiency. In this context fin efficiencies refer to the efficiency of the heat transfer in the components. Fin efficiencies for the cooling air in the fuel cell and the heating air in the evaporator also have to be made.

It is, unfortunately, not possible to measure the exhaust temperatures independently and an empirical approach has, therefore, been employed. In a series of identification experiments the module is operated with a series of constant fuel cell currents. The mass flows of the cooling air are then calculated on the basis of the blower PWM signals and the blower models. Knowing that the temperature is constant, the sum of the heating powers in Eqs. (4) and (5) must be equal to zero and the electric heater is off. This yields the following expression for the cooling flow:

$$\dot{Q}_{\text{air},b} = \dot{Q}_{\text{H}_2,b} + \dot{Q}_{\text{CH}_3\text{OH},b} - \dot{Q}_{h,r} - \dot{Q}_{\text{reform}} - \dot{Q}_{c,r} - \dot{Q}_{\text{heat},b} \tag{13}$$

All of the powers on the right-hand side of the equation can be calculated using the models presented earlier in this work and the actual cooling power can, therefore, be calculated. Fin efficiency models can thereby be constructed using linear regression. A model which uses the maximum cooling power and the maximum cooling power squared as inputs are found to have the best fit. This model displays an MAE of 6.2%, which is higher than most of the MAE errors recorded in this work. This is most likely because of the many calculated variables in Eq. (13).

A similar model is constructed for the fuel cell fin efficiency using the fact that, in steady state, the powers in Eq. (6) equal 0 and the electric heater is off

$$\dot{Q}_{\text{air,FC}} = P_{\text{loss,FC}} - \dot{Q}_{h,\text{FC}} - \dot{Q}_{c,\text{FC}} \tag{14}$$

Again, a model which uses the maximum cooling power and the maximum cooling power squared proves to give the best fit. The MAE is 1.12%, which is deemed to be acceptable. By knowing the cooling power in the fuel cell, the temperature of the fuel cells exhaust air can be calculated. This is then used to construct a model of the fin efficiency of the evaporator using a similar method. A model which is dependent on the maximum heating power and the maximum heating power squared is found to have the best performance. Here, the MAE is 0.98%.

2.6 Heat Exchanger. The primary purpose of the heat exchanger is to channel the gas flows between the components of the system. In addition, it is used to transfer heat from the reformed gas and the fuel cell anode exhaust to the evaporated fuel. The lack of temperature measurements in the heat exchanger means that it is difficult to model the heat transfer between the gas flows, but the channels are only a few cm long and their effect is, therefore, expected to be small. Therefore, the thermal transfer rates are set to low values. The experiments seem to confirm this, but measurements of the flow temperatures in and out of the heat exchanger would make it possible to improve the heat exchanger model in the future.

2.7 Model Overview. The models presented in the previous sections of this work are combined into a dynamic MATLAB Simulink model. Figure 7 shows an overview of this model.

The model is divided into a series of subsystems representing each component of the H3-350 module. The subsystems contain the various thermal and electrical models described in the previous sections. The inputs to the model are the externally controllable factors, which are: the blower PWM signals, the fuel pump set point, the power for the electric heaters, and the fuel cell current set point. This means that the controllers developed using the model will have the exact same outputs as the controllers which are to be implemented in the H3-350 module. The temperatures, which can be measured in the real system, are logged in the simulation for comparison as along with some temperatures and flows which cannot be measured. These can then be used to analyze the performance of the module in a more detailed way than what is possible without a model.

3 Model Validation

The validity of the models developed in this work is assessed in this section. First, the MAEs of the individual models are summarized and then the performance of the complete model is evaluated.

The MAE of the models presented in this paper are summed up in Table 1.

As the table shows, most of the models have MAEs below 5%. The exceptions are the carbon monoxide mass model and the burner fin efficiency model. The relatively high MAE of the carbon monoxide model is due to noise in the measurements. That of the burner fin efficiency model is most likely due to the many calculated variables in Eq. (13) upon which it is based.

To investigate the validity of the dynamic model, a series of load changes are performed on the H3-350 module and replicated in the dynamic MATLAB Simulink model. In the experiment the fuel cell current, which is the controllable parameter, starts at 14 A and is then stepped to 10 A, then back to 14 A, and, finally, up to 16 A. These operating points are chosen because they span the entire operating range of the module. Figure 8 shows the fuel

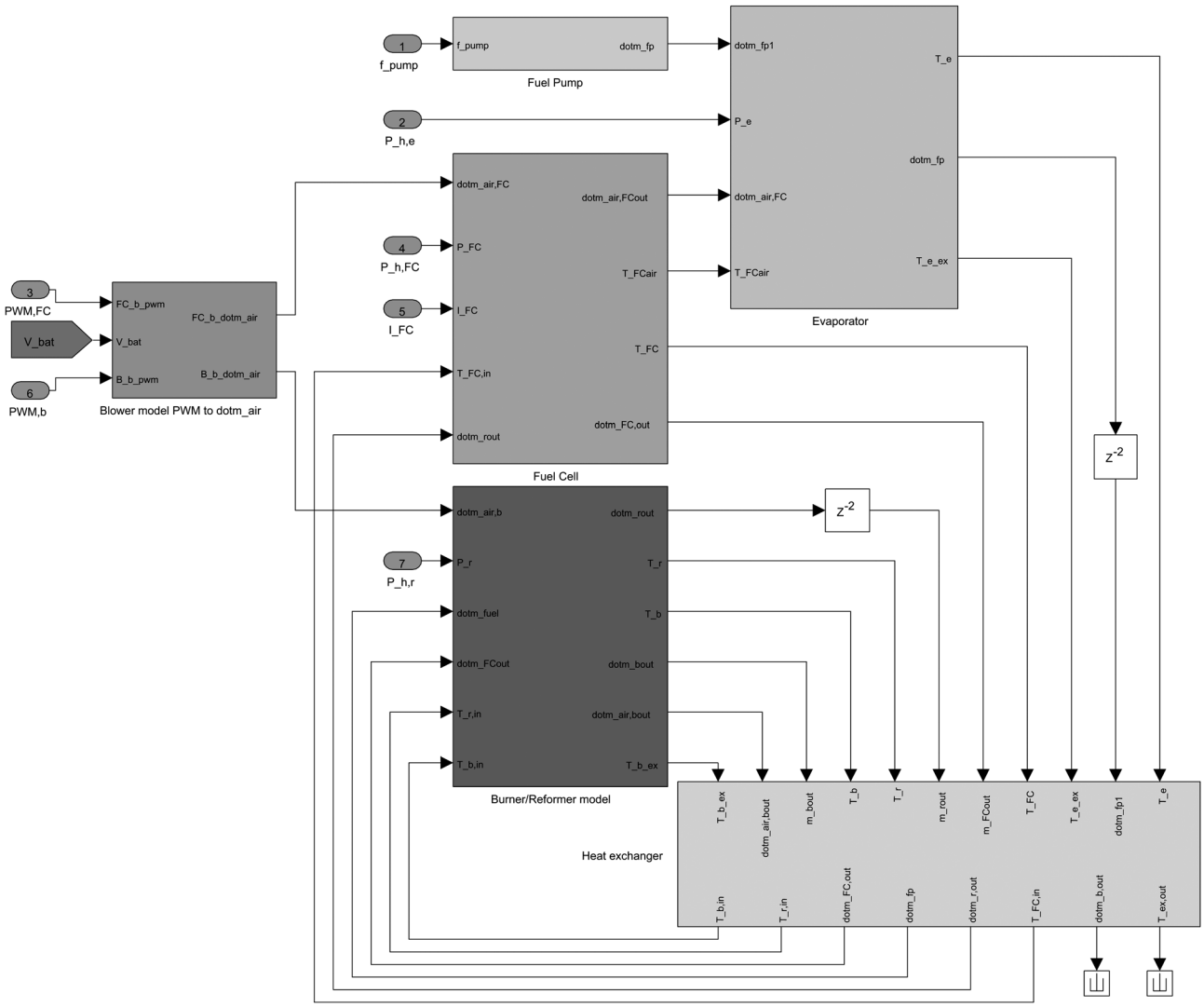

Fig. 7 Screen shot of the model implemented in Matlab Simulink

Table 1 The mean absolute errors (MAEs) of the models presented in this work

Model	MAE (%)
Hydrogen mass flow	0.70
Carbon dioxide mass flow	0.71
Carbon monoxide mass flow	6.4
Methanol mass flow	4.56
Fuel cell blower speed model	1.17
Burner blower speed model	0.98
Fuel cell blower mass flow model	1.44
Burner blower mass flow model	3.9
Total blower mass flow model	2.10
Fuel cell voltage model	0.4
Burner fin efficiency model	6.2
Fuel cell fin efficiency model	1.12
Evaporator fin efficiency model	0.98

cell current, fuel cell temperature, and reformer temperature during the experiment and the simulation.

The fuel cell temperature of the model and the experiment are very similar through all of the load changes. The amplitude and frequency of the oscillations are similar and the thermal model of the fuel cell is considered valid.

The oscillations in the reformer temperature of the model and the experiments also have some similarities when it comes to the amplitude and frequency of the oscillations. There are, however, some differences. When a positive step in the fuel cell current is performed, the reformer temperature in the model drops due to the larger fuel flow into the reformer at this operating point. In the experiment the temperature increases a little and then drops. This is most likely due to the fact that the burner and reformer are modeled as thermal masses with no internal temperature gradients. In the H3-350 module the temperature sensor is placed in the bulk material next to the reformer but between the burner and the reformer, as illustrated in Fig. 9.

The delay before the reformer temperature drops is most likely due to the time it takes for the cooling effect to reach the sensor. The larger drop in the reformer temperature after the short increase is most likely due to integrator windup in the temperature controller achieved during the short increase in reformer temperature. The reformer and burner models are considered to be valid for controller design even though they display some differences compared with the experimental results. This is because the oscillations in the model are similar in amplitude and frequency to those of the experiment.

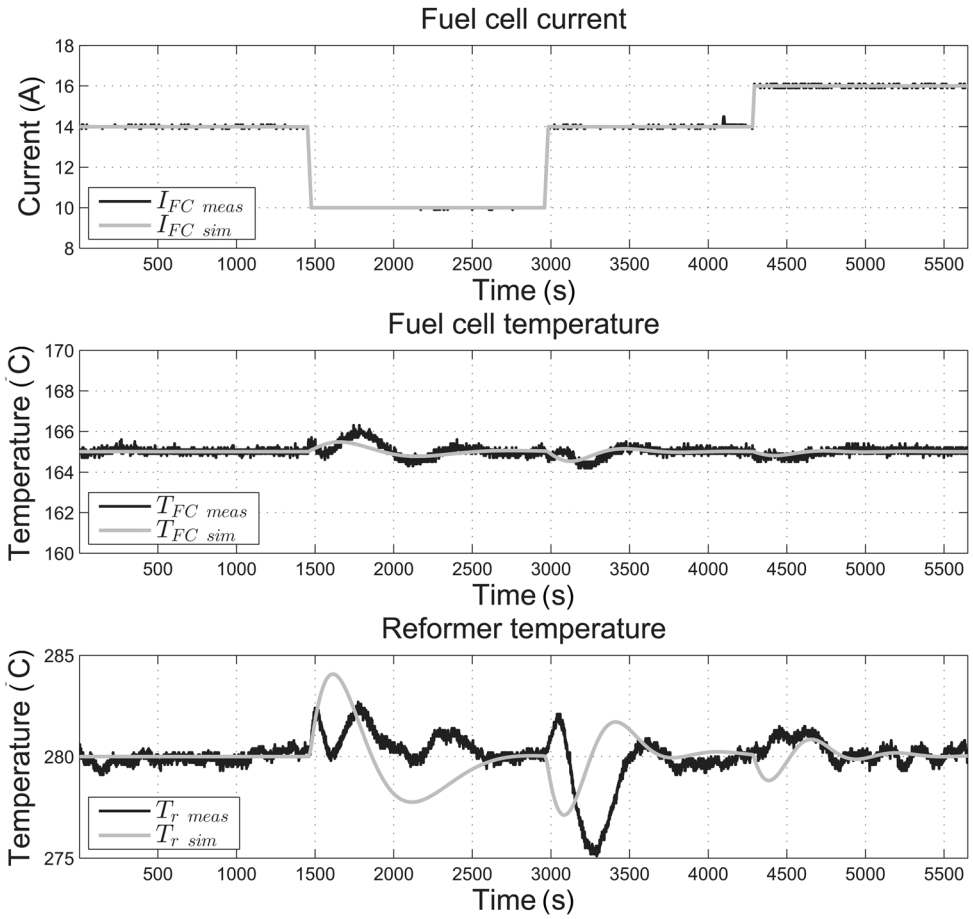

Fig. 8 Comparison of the response of the model and the real system to the same change in fuel cell current

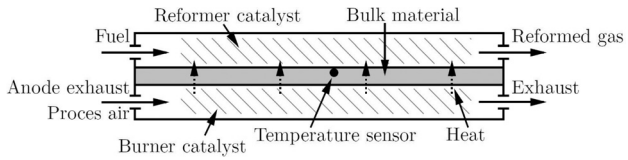

Fig. 9 Illustration of a possible explanation for the drop in temperature observed in the model but not in the experiments

4 Conclusion

A dynamic MATLAB Simulink model of an H3-350 reformed methanol fuel cell module produced by Serenergy® has been developed in this work. The purpose of this model is to aid in the design of the controllers for the module and analyze the internal unmeasurable states of the module.

The components of the module have been modeled as lumped thermal masses and adaptive neuro-fuzzy inference system models of the gas composition have been presented. Blower models and fin efficiency models have been constructed using a series of physical and empirical methods such as linear regression. A fuel cell model has been constructed based on a modified version of the one presented in Ref. [10]. The accuracy of the individual parts of the model has been individually verified as part of the design process. Finally, the functionality of the model has been demonstrated by comparing the results of the simulations with the results of the experiments performed on the module.

It is concluded that the model is valid for the purpose of controller design and for the analysis of the internal unmeasurable states of the module, even though there are some differences when the reformer temperature is observed. Some of the models, such as those of the fin efficiencies and the gas composition, are empirical models. This means that they cannot be used to analyze the effect of physical changes to the module.

5 Future Work

Several steps can be taken to improve the accuracy of the models. The fuel cell will change performance characteristics over time and this could be included in the model. This also applies to the reformer, which is important because it leads to a lower rate of fuel reforming and thereby, a lower hydrogen production. This introduces a risk of fuel cell anode starvation if measures are not taken to keep the anode stoichiometry constant.

The parameters of the heat exchanger model would benefit from tuning based on measurements of the flow temperatures in and out of the heat exchanger, which are not currently available.

A new version of the H3-350 module is being developed by Serenergy® which has a slightly different construction. The model could be adapted to fit this new version.

Acknowledgment

We gratefully acknowledge the financial support from the EUDP program and the Danish Energy Agency. The cooperation of Serenergy® is greatly appreciated and, furthermore, we would like to acknowledge the work carried out by Mikkel P. Ehmsen, John Andersen, and Simon L. Sahlin related to the early parts of the modeling and experimental work.

References

[1] Serenergy A/S home page, http://www.serenergy.com/
[2] Amphlett, J. C., Creber, K. A. M., Davis, J. M., Mann, R. F., Peppley, B. A., and Stokes, D. M., 1994, "Hydrogen Production by Steam Reforming of

Methanol for Polymer Electrolyte Fuel Cells," Int. J. Hydrogen Energy, **19**(2), pp. 131–137.
[3] Chrenko, D., Gao, F., Blunier, B., Bouquain, D., and Miraoui, A., 2010, "Methanol Fuel Processor and PEM Fuel Cell Modeling for Mobile Application," Int. J. Hydrogen Energy, **35**, pp. 6863–6871.
[4] Chang, H., Cheng, S.-H., Chiang, H.-C., Chen, Y.-H., and Chang, Y.-Y., 2012, "Simulation Study of an Integrated Methanol Micro Fuel Processor and Fuel Cell System," Chem. Eng. Sci., **74**, pp. 27–37.
[5] Andreasen, S. J., Vang, J. R., and Kær, S. K., 2011, "High Temperature PEM Fuel Cell Performance Characterisation With CO and CO_2 Using Electrochemical Impedance Spectroscopy," Int. J. Hydrogen Energy, **36**, pp. 9815–9830.
[6] Li, Q., Jensen, J. O., Savinell, R. F., and Bjerrum, N. J., 2009, "High Temperature Proton Exchange Membranes Based on Polybenzimidazoles for Fuel Cells," Prog. Polym. Sci., **34**, pp. 449–477.
[7] Zhang, J., Xie, Z., Zhang, J., Tang, Y., Songa, C., Navessin, T., Shi, Z., Song, D., Wang, H., Wilkinson, D. P., Liu, Z.-S., and Holdcroft, S., 2006, "High Temperature PEM Fuel Cells," J. Power Sources, **160**, pp. 872–891.
[8] Jang, J.-S. R., 1993, "ANFIS: Adaptive-Network-Based Fuzzy Inference System," IEEE Trans. Syst. Man Cybern., **23**, pp. 665–685.
[9] Justesen, K. K., Andreasen, S. J., Shaker, H. R., Ehmsen, M. P., and Andersen, J., 2013, "Gas Composition Modeling in a Reformed Methanol Fuel Cell System Using Adaptive Neuro-Fuzzy Inference Systems," Int. J. Hydrogen Energy, **38**, pp. 10577–10584.
[10] Korsgaard, A. R., Nielsen, M. P., Bang, M., and Kær, S. K., 2006 "Modeling of CO Influence in PBI Electrolyte PEM Fuel Cells," ASME 2006 4th International Conference on Fuel Cell Science, Engineering and Technology, Irvine, CA, June 19–21, ASME Paper No. FUELCELL2006-97214.